T2R2 東京科学大学 リサーチリポジトリ
Science Tokyo Research Repository

論文 / 著書情報
Article / Book Information

Title	Significance of PGR5-dependent cyclic electron flow for optimizing the rate of ATP synthesis and consumption in Arabidopsis chloroplasts
Authors	Ryoichi Sato, Rinya Kawashima, Mai Duy Luu Trinh, Masahiro Nakano, Takeharu Nagai, Shinji Masuda
Citation	Photosynthesis Research, pp. 1–7
Pub. date	2018, 6
Note	This is a post-peer-review, pre-copyedit version of an article published in Photosynthesis Research. The final authenticated version is available online at: http://dx.doi.org/10.1007/s11120-018-0533-9.

Powered by T2R2 (Science Tokyo Research Repository)

Manuscript

Click here to download Manuscript
Revised_MS_LANTRN.docx

Click here to view linked References

Significance of PGR5-dependent cyclic electron flow for optimizing the rate of ATP synthesis and consumption in Arabidopsis chloroplasts

Ryoichi Sato[1,4], Rinya Kawashima[1], Mai Duy Luu Trinh[1], Masahiro Nakano[2], Takeharu Nagai[2], and Shinji Masuda[3,*]

[1]School of Life Science and Technology, Tokyo Institute of Technology, Yokohama 226-8501, Japan

[2]The Institute of Scientific and Industrial Research, Osaka University, Osaka 567-0047, Japan

[3]Center for Biological Resources & Informatics, Tokyo Institute of Technology, Yokohama 226-8501, Japan

[4]Present address: Division of Environmental Photobiology, National Institute for Basic Biology, Okazaki 444-8585, Japan

*Corresponding author: shmasuda@bio.titech.ac.jp

Abstract The proton motive force (PMF) across the chloroplast thylakoid membrane that is generated by electron transport during photosynthesis is the driving force for ATP synthesis in plants. The PMF mainly arises from the oxidation of water in photosystem II and from electron transfer within the cytochrome b_6f complex. There are two electron transfer pathways related to PMF formation: linear electron flow and cyclic electron flow. Proton gradient regulation 5 (PGR5) is a major component of the cyclic electron flow pathway, and the Arabidopsis *pgr5* mutant shows a substantial reduction in the PMF. How the PGR5-dependent cyclic electron flow contributes to ATP synthesis has not, however, been fully delineated. In this study, we monitored *in vivo* ATP levels in Arabidopsis chloroplasts in real time using a genetically encoded bioluminescence-based ATP indicator, Nano-lantern(ATP1). The increase in ATP in the chloroplast stroma of *pgr5* leaves upon illumination with actinic light was significantly slower than in wild type, and the decrease in ATP levels when this illumination stopped was significantly faster in *pgr5* leaves than in wild type. These results indicated that PGR5-dependent cyclic electron flow around photosystem I helps to sustain the rate of ATP synthesis, which is important for growth under fluctuating light conditions.

Keywords Photosynthesis, PGR5, ATP indicator, Nano-lantern, cyclic electron flow, chloroplast

Introduction

Photosynthesis, which occurs in chloroplasts, captures the energy of visible light and converts it into chemical energy, thereby providing energy for most life forms on Earth. Specifically, the photochemical reaction occurs in the thylakoid membranes of the chloroplast, the interior of which has two compartments, the lumen and the stroma, in which the oxidation of water and assimilation of carbon dioxide occur, respectively. During photosynthesis, electrons are transferred in turn from photosystem II (PSII) to plastoquinone, the cytochrome b_6f complex, plastocyanin, photosystem I (PSI), and ultimately to ferredoxin. Two reduced ferredoxin molecules each donate one electron to ferredoxin-$NADP^+$ oxidoreductase to reduce a single molecule of $NADP^+$, thereby producing NADPH. This electron transfer process is referred to as linear electron flow. As a consequence of the oxidation of water in PSII and photosynthetic electron transfer through the cytochrome b_6f complex, H^+ accumulates on the luminal side of chloroplasts, which generates the proton motive force (PMF) composed of a proton gradient across the thylakoid membrane (ΔpH) and a membrane potential (ΔΨ). In turn, ΔpH and ΔΨ equally contribute to ATP synthesis by plastidial ATP synthase embedded in thylakoid membranes. Synthesized NADPH and ATP are used to fix carbon dioxide in the Calvin-Benson cycle in the chloroplast stroma (Blankenship 2002).

A second pathway for electron flow, the so-called cyclic electron flow (CEF), also contributes to the formation of ΔpH in chloroplasts, with electrons being returned to plastoquinone from reduced ferredoxin (Shikanai 2007). In higher plants, two CEF pathways are known: the proton gradient regulation 5 (PGR5)-dependent pathway and the NADH dehydrogenase–dependent pathway (Shikanai 2016; Shikanai and Yamamoto 2017). In C3 plants,

the contribution of PGR5-dependent CEF for PMF formation is believed to be much larger than that of the NADH dehydrogenase–dependent pathway (Shikanai 2016), although its mechanism is still debated (Avenson et al. 2005; Suorsa et al. 2016; Shikanai 2016). We recently used quenching of aminoacridine to directly measure ΔpH formation and showed that the contribution of PGR5-dependent CEF to the total ΔpH formation is ~30% in Arabidopsis chloroplasts (Kawashima et al. 2017). However, the contribution of PGR5-dependent CEF for ATP synthesis has not been studied.

To characterize the dynamics of biological molecules during various biological processes, different types of indicator proteins have been developed (Saito and Nagai 2015; Suzuki and Nagai 2017). For example, fluorescence-based Ca^{2+} indicators have been used to monitor Ca^{2+} flux in mammalian cells and in plant tissues and have provided crucial information about the control of ion dynamics across different time scales and about the involvement of calcium ions in various physiological phenomena (Wu et al. 2013; Miyawaki et al. 1999; Horikawa et al. 2010; Zhao et al. 2011; Ohkura et al. 2012; Akerboom et al. 2013; Iwano et al. 2015). However, fluorescent protein–based indicators cannot be easily applied to the study of light-dependent biological processes, including photosynthesis, because the chlorophyll in green plant tissues autofluoresces. The development of bioluminescent protein–based indicators that do not require light illumination for observation has overcome this problem (Saito and Nagai 2015). Saito and colleagues developed the bright bioluminescent protein Nano-lantern, whose emission intensity is enhanced by an efficient intramolecular Forster resonance energy transfer from RLuc(S273G), an enhanced *Renilla* luciferase, to Venus, a yellow fluorescent protein (Saito et al. 2012). They also created the Nano-lantern–based ATP indicator

Nano-lantern(ATP1), which harbors the ATP-binding ε subunit of the bacterial F_OF_1-ATP synthase and exhibits a 200% increase in light output upon ATP binding to the domain (Saito et al. 2012). Nano-lantern(ATP1) allows the assessment of alterations in ATP levels *in vivo* during changes in the light environment under conditions in which fluorescence protein–based indicators cannot be used.

Here we used Nano-lantern(ATP1) to determine the contribution of PGR5-dependent CEF to ATP synthesis *in vivo*. We introduced a recombinant Nano-lantern(ATP1) gene into chloroplasts of wild-type (WT) Arabidopsis and the *pgr5* mutant and then monitored ATP dynamics in real time in the presence and absence of actinic light. We found that the increase and decrease in photon emission from Nano-lantern(ATP1) upon turning the actinic light on and off, respectively, were slower and faster, respectively, in the *pgr5* mutant than in WT, which indicated that the PGR5-dependent CEF contributes to the optimization of ATP synthesis and consumption under conditions of fluctuating light intensity.

Materials and Methods

Plants and growth conditions

Wild-type *Arabidopsis thaliana* (Columbia) and the *pgr5* mutant (Munekage et al. 2002) were grown on Murashige and Skoog medium containing 0.8% (w/v) agar or in soil at 23°C under constant illumination (40–50 μmol photons m^{-2} s^{-1}).

Construction of recombinant plants

The DNA fragment encoding the N-terminal chloroplast transit peptide of Arabidopsis RecA (At1g79050) was PCR-amplified with the primer pair 5′-CACTGTTGATACATATGGATTCACAGCTAGTCTTGTCTCTG-3′ and 5′-GCCCTTGCTCACCATGTCGCGATCGAATTCAGAACTGATTTTG-3′ from Arabidopsis genomic DNA. The DNA fragment encoding Nano-lantern(ATP1) (Saito et al. 2012) was PCR-amplified with the primer pair 5′-CACTGTTGATACATATGGTGAGCAAGGGC-3′ and 5′-ATTCAGAATTGTCGACTTACTGCTCGTTCTTCAGC-3′ from plasmid DNA encoding the Nano-lantern(ATP1). The two amplified fragments were mixed and cloned into *Nde*I- and *Sal*I-digested pRI201 vector (TaKaRa) using In-Fusion Cloning reagent (Clontech). The resulting plasmid was transformed into WT Arabidopsis and the *pgr5* mutant using the standard Agrobacterium-based transformation method. The transformants were selected on Murashige and Skoog medium containing 10 mg L^{-1} kanamycin. T2-generation plants were used for imaging and other analyses as described (Saito et al. 2012).

To ensure that Nano-lantern luciferase activity was present in the recombinant plants, ~0.1 ml of 100 μM coelenterazine h (Promega) or solvent (16% [v/v] methanol) was injected, using a 1-ml plastic syringe (Terumo) into leaves detached from the recombinant plants. After incubation for ~1 min, luminescence in the leaves was imaged with the use of an ImageQuant LAS 500 luminescent imager (GE Healthcare). Expression of Nano-lantern(ATP1) was also assessed by western blotting as follows. Leaves from each recombinant plant were homogenized in 50 mM Tris-HCl (pH 6.8), 10% (v/v) glycerol, 5% (v/v) β-mercaptoethanol and 2.5% (w/v) sodium dodecyl sulfate (SDS). The homogenized samples were boiled for 5 min and then centrifuged at 15,000 × *g* for 5 min. Proteins in the supernatant were separated by

SDS-polyacrylamide gel electrophoresis. After electrophoresis, proteins were electroblotted onto a polyvinylidene fluoride membrane (GE Healthcare). Membrane-bound proteins were immunoprobed with an antibody against green fluorescent protein (anti-GFP; Living Colors A.v. monoclonal antibody JL-8, Clontech) and detected using ECL Advance Blotting Detection kit reagents (GE Healthcare).

Measurement of chlorophyll fluorescence

Chlorophyll fluorescence was measured using an IMAGING_PAM chlorophyll Fluorometer (MAXI-versions; Walz, Effeltrich, Germany) in leaves attached to 7-day-old plants after 30 min of dark adaptation. The flux density of the applied actinic light was 80 μmol m^{-2} s^{-1} (λ_{max} = 450 nm). Each non-photochemical-quenching (NPQ) value was calculated as $(F_m - F_m')/F_m'$, where F_m is the maximum chlorophyll fluorescence after dark adaptation and F_m' is the maximum fluorescence yield in illuminated samples.

Localization of Nano-lantern(ATP1) determined by fluorescence microscopy

Arabidopsis *pgr5* mutants expressing recombinant Nano-lantern(ATP1) were grown in soil for 4 weeks under continuous light, and then the Venus and chlorophyll fluorescence in their rosette leaves was visualized by confocal laser scanning microscopy (LSM780, Zeiss).

Microscopic analysis for visualizing ATP synthesis *in vivo*

Wild-type Arabidopsis and *pgr5* mutants expressing recombinant Nano-lantern(ATP1) were grown in Murashige and Skoog medium, and the first or second leaves of 7-day-old plants were

harvested. Detached leaves were injected with coelenterazine h as described above and then, to assess their luminescence, were immediately placed onto the stage of a microscope system (Ti-E (Nikon), which included a camera, iXon Ultra 897 (Andor Technology); objective lens, CFI Plan Apo VC 20× (NA = 0.75) (Nikon) and filters, FF02-438/24 (actinic light, Semrock), FF01-500/24 (mVenus excitation, Semrock) and FF01-542/27 (mVenus emission, Semrock). The settings were as follows: exposure, 1 s; dead time, 300 ms; binning, 1; EMgain, Max. The luminescence in the leaves was measured in the presence and absence of actinic light (λ_{max} = 438 nm; 9.1 mW cm^{-2}).

Rise and decay signals over a 7-s period were acquired immediately after dark-to-light or light-to-dark transitions and then were fit to single exponential curves. The luminescence rise and decay rates are reported herein as the half-life of each exponential curve. We performed at least three replicates for each analysis.

Results and Discussion

To cause Nano-lantern(ATP1) to localize into chloroplast stroma, we genetically fused the transit peptide of Arabidopsis plastidial RecA to the N terminus of Nano-lantern(ATP1). The recombinant gene was placed downstream of the cauliflower mosaic virus 35S promoter, and the construct was separately introduced into WT Arabidopsis and *pgr5* mutant plants. First, we determined the location of expressed Nano-lantern(ATP1) by confocal fluorescence microscopy. Venus-derived yellow fluorescence in WT leaves expressing Nano-lantern(ATP1) clearly overlapped with chlorophyll fluorescence (Fig. 1a), indicating that the transit peptide of RecA had directed Nano-lantern(ATP1) into chloroplasts. Direct expression of Nano-lantern(ATP1)

was verified by western blotting. The calculated molecular weight of Nano-lantern(ATP1), according to its deduced amino-acid sequence minus the transit peptide, is ~77 kDa. Proteins from the leaves of several independently transformed plants were subjected to western blotting. Four WT plants (lines 1, 2, 3 and 4) and three *pgr5* plants (lines 1, 3 and 4) expressed Nano-lantern(ATP1) (Supplemental Fig. S1a). We also determined if the luciferase activity associated with Nano-lantern(ATP1) was present in these lines. Bioluminescence was clearly detected in leaves of recombinant plants in which the luciferase substrate coelenterazine h had been injected, but not in those of negative controls (Supplemental Fig. S1b), which indicated that luciferase in the introduced Nano-lantern(ATP1) was active.

We also determined whether expression of Nano-lantern(ATP1) affected photosynthetic activity. As observed previously in the first *pgr5* mutant constructed (Munekage et al. 2002), NPQ induction upon a dark-to-light transition in two Nano-lantern(ATP1)-expressing *pgr5* mutants constructed for this study (lines 1 and 3; Supplemental Fig. S1a) was strongly suppressed compared with the WT plants (Supplemental Fig. S2). Notably, the two *pgr5* recombinants had nearly identical NPQ induction kinetic profiles (Supplemental Fig. S2). NPQ involves multiple reactions including a pH-regulated energy dissipation mechanism in the PSII antenna proteins (referred to as qE), state transitions and photoinhibition, with qE being the major component of NPQ in land plants; qE is induced by acidification of the thylakoid lumen, which is accelerated by photosynthetic electron transport (Ruban 2016). These results indicated that the presence of Nano-lantern(ATP1) and its activity did not influence photosynthetic electron transport.

To monitor ATP synthesis *in vivo*, we injected coelenterazine h into 7-day-old leaves of the recombinant WT and mutant plants, immediately placed the injected leaves under a microscope and looked for the bioluminescence signal from Nano-lantern(ATP1) in those leaves in the presence and absence of actinic light. We used blue light (λ_{max} = 438 nm) to drive photosynthesis, because its maximum wavelength does not overlap that of the Nano-lantern signal (~540 nm). A clear bioluminescence signal was observed when the coelenterazine h–injected leaves were illuminated with actinic light (Fig. 1b, Light). Because such bioluminescence was not detected when the leaves were placed in the dark (Fig. 1b, Dark), the bioluminescence indicated only ATP synthesis driven by photosynthetic electron transfer. The bioluminescence overlapped the Venus fluorescence, which showed plastidial localization (Fig. 1b, Venus), thus indicating that ATP in chloroplast stroma was detected as bioluminescence from the introduced Nano-lantern(ATP1), as reported previously (Saito et al. 2012). Because this bioluminescence intensity varies depending on the Nano-lantern content, the level of which cannot be precisely controlled in a plant, the absolute amounts of ATP cannot be quantified by this method, although it does allow monitoring of the kinetics of ATP synthesis in real time.

We then analyzed the kinetics of luminescence intensity induced by 25-s actinic light/15-s dark cycles. Clear bioluminescence induction was observed when coelenterazine h–injected leaves were irradiated with actinic light, and the bioluminescence dropped to the background level after the actinic light was turned off (Fig. 2, WT; Supplementary movie 1). Similar induction kinetics were also observed during a second round of illumination. The negative controls (coelenterazine h–injected leaves of WT plants that had not been transformed with Nano-lantern(ATP1)) did not show such bioluminescence induction (Fig. 2, gray line),

indicating that ATP synthesis in chloroplast stroma can be visualized by monitoring the bioluminescence kinetics of Nano-lantern(ATP1).

Similar induction of Nano-lantern(ATP1) bioluminescence was observed in the leaves of *pgr5* mutants (Fig. 2, *pgr5*). Specifically, a sharp rise immediately after irradiation with actinic light that was followed by a gradual increase in the signal was also observed in the leaves of Nano-lantern(ATP1)–expressing *pgr5*. Using the observed kinetics, the half-life of the light-driven increase in the bioluminescence signal upon a dark-to-light transition could be calculated, and the calculated values indicated that the bioluminescence increases in the leaves of *pgr5* mutants were significantly retarded compared with WT, especially during the second round of illumination (Fig. 3a). The bioluminescence decrease found after turning off the actinic light was significantly faster in *pgr5* than in WT (Fig. 3b). Both findings indicate that ATP synthesis must have been slower and/or ATP consumption faster in *pgr5* than in WT. Attenuation of ATP synthesis is the more probable event, because PGR5 is an important component of PSI-dependent CEF, and formation of ΔpH across the thylakoid membranes is abnormal in the *pgr5* mutant (Shikanai 2016, Kawashima et al. 2017).

What is the physiological role(s) of PGR5-dependent control of ATP synthesis and consumption rates? In nature, plants experience dynamic fluctuations in light intensity because of movements of clouds that shade the plants from sunlight. Plants in canopies also experience fluctuations in light caused by wind-driven movements of leaves and stems in plants higher up, a phenomenon called sunflecks (Pearcy 1990; Koizumi and Oshima 1993; Vierling and Wessman 2000; Smith and Berry 2013). In the understory, a leaf may receive only a few sunflecks on one day but could receive up to 300 sunflecks on another day. Most sunflecks last

<10 s, and only ~1% of those are long enough to induce a full photon flux density. Plants use two strategies to maintain photosynthesis under sunfleck conditions: one is to increase the photosynthetic rate almost instantaneously when exposed to an increase in light intensity, and the other is to maintain carbon assimilation as long as possible after initiation of sunflecks (Way and Pearcy 2012; Smith and Berry 2013). These sophisticated systems could allow plants to use 10 to 60% of the total energy in sunflecks for carbon assimilation per day (Pearcy 1990; Way and Pearcy 2012). Given that the *pgr5* mutant had a slower rate of ATP synthesis upon a dark-to-light transition and a faster rate of ATP consumption upon light-to-dark transition than did WT (Fig. 3), a PGR5-dependent CEF might contribute to keeping photosynthesis rate during the transition when sunflecks occur.

Regulation of ATP synthesis via CEF around PSI is also important to minimize photodamage and maximize repair of PSII (Allakhverdiev et al. 1997; Huang et al. 2010; Huang et al. 2018). Specifically, photo-inhibited PSII, caused by strong light stress, recovers rapidly under less-intense light owing to the fast turnover rate of the PSII reaction center protein D1 (Aro et al. 1993; Zhang and Scheller 2004; Allakhverdiev 2011), and a certain amount of stromal ATP is needed for this light-dependent repair of PSII complexes (Mattoo et al. 1984; Kuroda et al. 1992; Allakhverdiev et al. 2005; Huang et al. 2010). This suggests that PGR5-dependent CEF regulates the repair of D1 and is likely to function as the ultimate control mechanism of photosynthetic electron transfer, allowing for maintenance of the PSI redox state (Tikkanen et al. 2014; Suorsa et al. 2016). Several mechanisms for regulation of D1 turnover through stromal ATP levels have been proposed, e.g., stromal ATP levels may regulate the translational elongation of D1 (Kuroda et al. 1992) and/or may be required for aminoacylation

of the cognate tRNA for translation of D1 (Allakhverdiev et al. 2005). However, the exact regulatory mechanism(s) is not fully understood, and the coordination of the rate of ATP synthesis, photodamage and repair of PSII remains to be investigated. The Nano-lantern(ATP1) imaging technique could be applied to elucidate explicitly the effect of ATP synthesis on photodamage and repair of PSII in plants and photosynthetic microorganisms.

In conclusion, we compared ATP dynamics in WT Arabidopsis and its *pgr5* mutant using images produced by Nano-lantern(ATP1), the results from which showed the importance of PGR5-dependent CEF for attenuation of ATP synthesis in response to changing light conditions. Although PGR5 had previously been shown to be involved in the control of NPQ and the photodamage response, this study is the first to directly show the role of PGR5-dependent CEF in the regulation of ATP synthesis and consumption under varying light conditions.

References

Akerboom J, Carreras Calderón N, Tian L, et al (2013) Genetically encoded calcium indicators for multi-color neural activity imaging and combination with optogenetics. Front Mol Neurosci 6:2.

Allakhverdiev SI (2011) Recent progress in the studies of structure and function of photosystem II. J Photochem Photobiol B Biol 104:1–8.

Allakhverdiev SI, Klimov V V., Carpentier R (1997) Evidence for the involvement of cyclic electron transport in the protection of photosystem II against photoinhibition: Influence of a Nnew phenolic compound. Biochemistry 36:4149–4154.

Allakhverdiev SI, Nishiyama Y, Takahashi S, et al (2005) Systematic analysis of the relation of electron transport and ATP synthesis to the photodamage and repair of photosystem II in Synechocystis. Plant Physiol 137:263–273.

Aro E-M, Virgin I, Andersson B (1993) Photoinhibition of Photosystem II. Inactivation, protein damage and turnover. Biochim Biophys Acta 1143:113–134.

Avenson TJ, Cruz JA, Kanazawa A, Kramer DM (2005) Regulating the proton budget of higher plant photosynthesis. Proc Natl Acad Sci 102:9709–9713.

Blankenship RE (2002) Molecular Mechanisms of photosynthesis. Blackwell Science Ltd

Horikawa K, Yamada Y, Matsuda T, et al (2010) Spontaneous network activity visualized by ultrasensitive Ca^{2+} indicators, yellow Cameleon-Nano. Nat Methods 7:729–732.

Huang W, Yang Y-J, Zhang S-B, Liu T (2018) Cyclic electron flow around photosystem I promotes ATP synthesis possibly helping the rapid repair of photodamaged photosystem II at low light. Front Plant Sci 9:239.

Huang W, Zhang S-B, Cao K-F (2010) Stimulation of cyclic electron flow during recovery after chilling-induced photoinhibition of PSII. Plant Cell Physiol 51:1922–1928.

Iwano M, Ito K, Fujii S, et al (2015) Calcium signalling mediates self-incompatibility response in the Brassicaceae. Nat Plants 1:15128.

Kawashima R, Sato R, Harada K, Masuda S (2017) Relative contributions of PGR5- and NDH-dependent photosystem I cyclic electron flow in the generation of a proton gradient in Arabidopsis chloroplasts. Planta. 246: 1045-1050.

Koizumi H, Oshima Y (1993) Light environment and carbon gain of understory herbs associated with sunflecks in a warm temperate deciduous forest in Japan. Ecol Res 8:135–142.

Kuroda H, Inagaki N, Satoh K (1992) The level of stromal ATP regulates translation of the D1 protein in isolated chloroplasts. Plant Cell Physiol 33:33–39.

Mattoo AK, Hoffman-Falk H, Marder JB, Edelman M (1984) Regulation of protein metabolism: Coupling of photosynthetic electron transport to in vivo degradation of the rapidly metabolized 32-kilodalton protein of the chloroplast membranes. Proc Natl Acad Sci 81:1380–1384.

Miyawaki A, Griesbeck O, Heim R, Tsien RY (1999) Dynamic and quantitative Ca^{2+} measurements using improved cameleons. Proc Natl Acad Sci U S A 96:2135–2140.

Munekage Y, Hojo M, Meurer J, et al (2002) PGR5 is involved in cyclic electron flow around photosystem I and is essential for photoprotection in Arabidopsis. Cell 110:361–371.

Ohkura M, Sasaki T, Kobayashi C, et al (2012) An improved genetically encoded red fluorescent Ca^{2+} indicator for detecting optically evoked action potentials. PLoS One 7:e39933.

Pearcy RW (1990) Sunflecks and photosynthesis in plant canopies. Annu Rev Plant Physiol Plant Mol Biol 41:421–453.

Ruban AV (2016) Nonphotochemical chlorophyll fluorescence quenching: Mechanism and effectiveness in protecting plants from photodamage. Plant Physiol 170:1903–1916.

Saito K, Chang Y-F, Horikawa K, et al (2012) Luminescent proteins for high-speed single-cell and whole-body imaging. Nat Commun 3:1262.

Saito K, Nagai T (2015) Recent progress in luminescent proteins development. Curr Opin Chem Biol 27:46–51.

Shikanai T (2007) Cyclic electron transport around photosystem I: Genetic approaches. Annu Rev Plant Biol 58:199–217.

Shikanai T (2016) Regulatory network of proton motive force: contribution of cyclic electron transport around photosystem I. Photosynth. Res. 129:253–260.

Shikanai T, Yamamoto H (2017) Contribution of cyclic and pseudo-cyclic electron transport to the formation of proton motive force in chloroplasts. Mol Plant 10:20–29.

Smith WK, Berry ZC (2013) Sunflecks? Tree Physiol 33:233–237.

Suorsa M, Rossi F, Tadini L, et al (2016) PGR5-PGRL1-dependent cyclic electron transport modulates linear electron transport rate in *Arabidopsis thaliana*. Mol Plant 9:271–288.

Suzuki K, Nagai T (2017) Recent progress in expanding the chemiluminescent toolbox for bioimaging. Curr Opin Biotechnol 48:135–141.

Tikkanen M, Mekala NR, Aro E-M (2014) Photosystem II photoinhibition-repair cycle protects Photosystem I from irreversible damage. Biochim Biophys Acta - Bioenerg 1837:210–215.

Vierling LA, Wessman CA (2000) Photosynthetically active radiation heterogeneity within a monodominant Congolese rain forest canopy. Agric For Meteorol 103:265–278.

Way DA, Pearcy RW (2012) Sunflecks in trees and forests: from photosynthetic physiology to global change biology. Tree Physiol 32:1066–1081.

Wu J, Liu L, Matsuda T, et al Improved orange and red Ca^{2+} indicators and photophysical considerations for optogenetic applications. ACS Chem Neurosci 19: 963-972.

Zhang S, Scheller HV (2004) Photoinhibition of photosystem I at chilling temperature and subsequent recovery in *Arabidopsis thaliana*. Plant Cell Physiol 45:1595–1602.

Zhao Y, Araki S, Wu J, et al (2011) An expanded palette of genetically encoded Ca^{2+} indicators. Science 333:1888–1891.

Figure legends

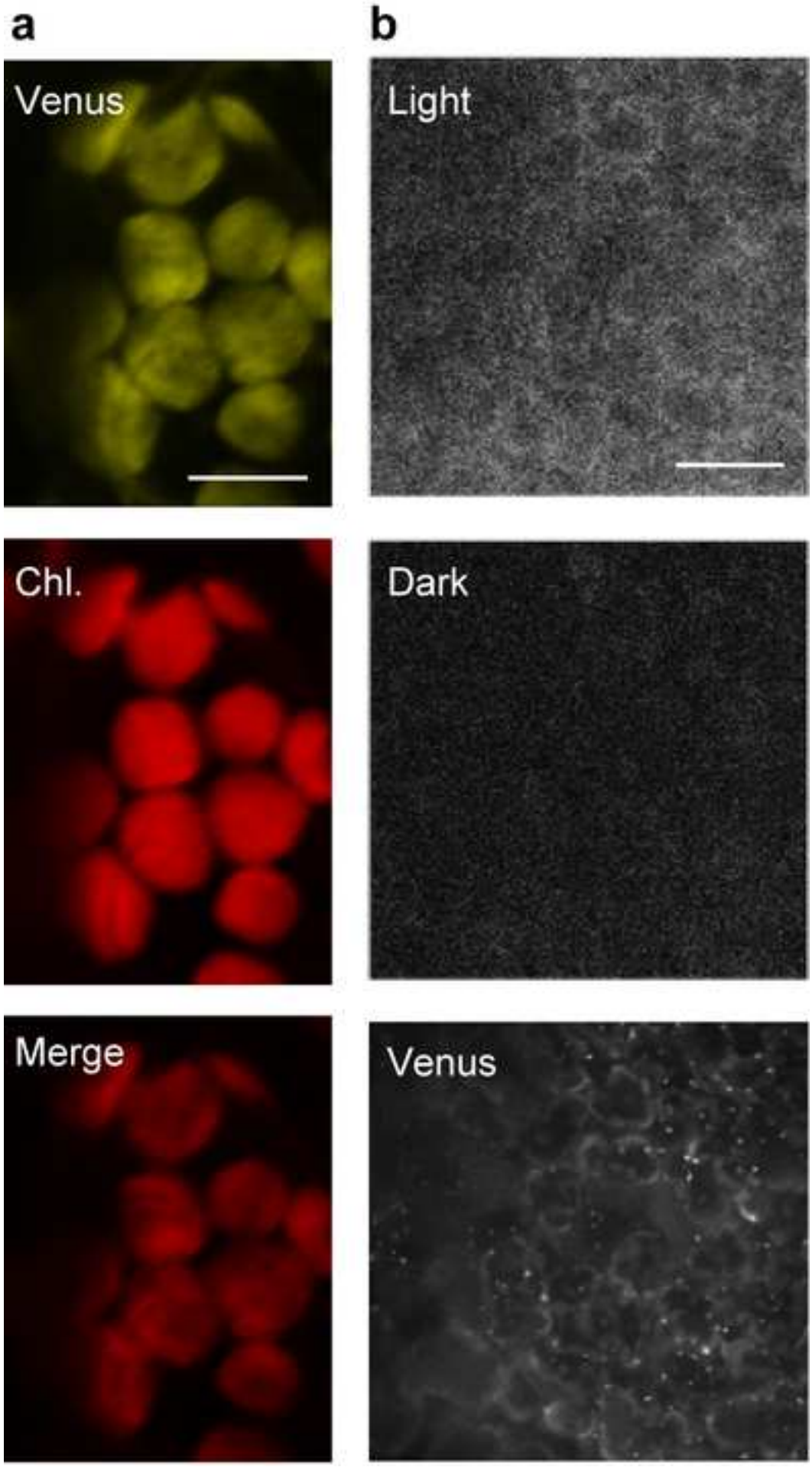
Fig. 1 Location of the introduced Nano-lantern(ATP1) and typical images of Nano-lantern(ATP1) signals in a leaf. **a** Venus- and chlorophyll (Chl)-derived fluorescence images of the leaf of a *pgr5* mutant expressing Nano-lantern(ATP1) as visualized by confocal fluorescence microscopy. Bar = 10 μm. **b** Bioluminescence images of the leaf from a WT plant expressing Nano-lantern(ATP1) (line 2: Supplemental Fig. S1a) under actinic light illumination (Light) and dark (Dark) conditions. A Venus-derived fluorescence image of the same leaf is shown in the panel labeled Venus. Bar = 100 μm.

Fig. 2 A typical time course of bioluminescence intensity changes in coelenterazine h–injected leaves of Nano-lantern(ATP1)–expressing WT (line 2: Supplemental Fig. S1a) and *pgr5* (line 1: Supplemental Fig. S1a) plants (black lines), and those of WT and *pgr5* plants that had not been transformed with Nano-lantern(ATP1) (gray lines). Bioluminescence was monitored under 25-s actinic light (9.1 mW cm^{-2})/15-s dark cycles.

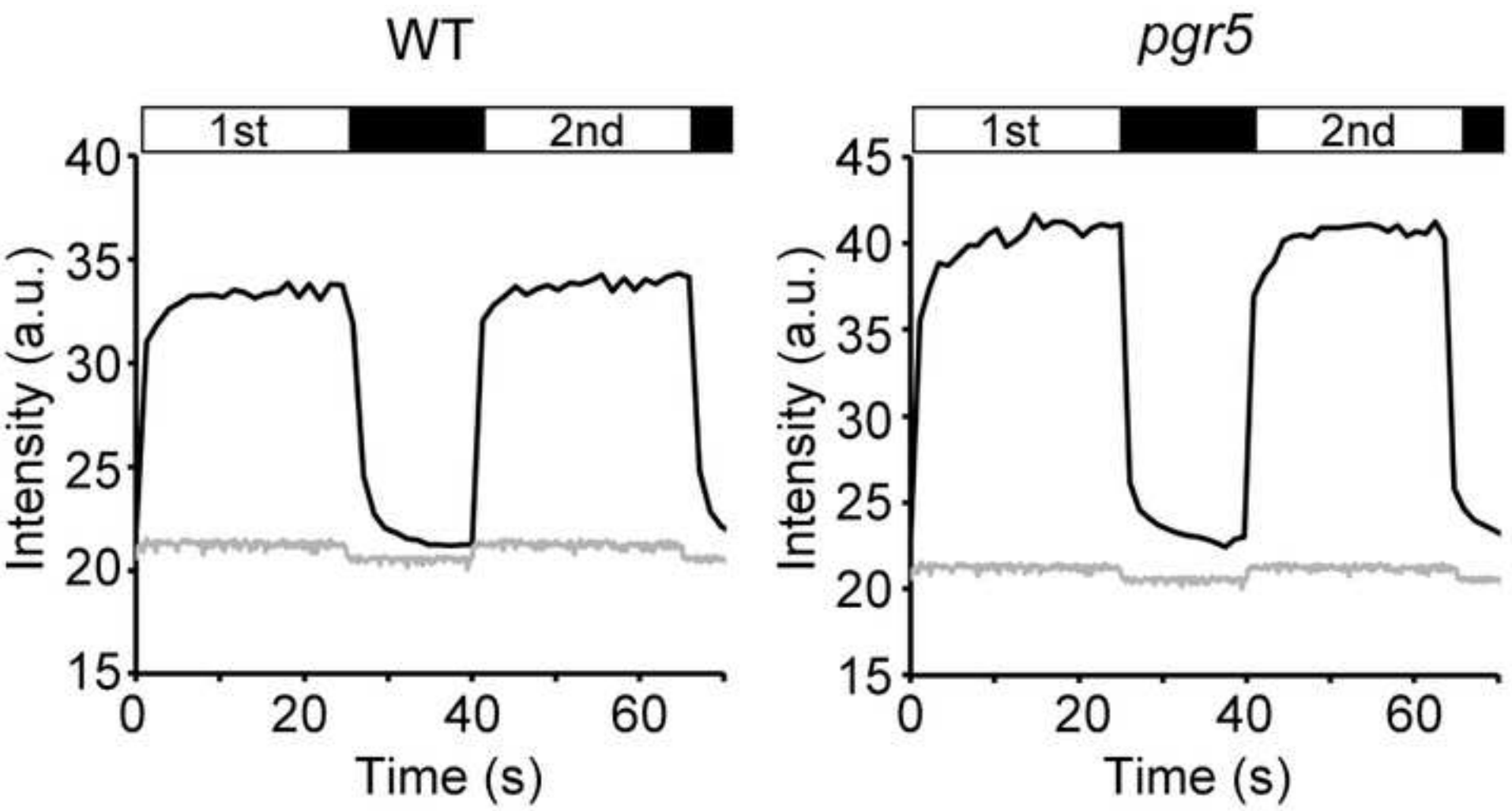
Fig. 3 Kinetics of ATP synthesis in *pgr5* mutant and WT leaves in response to actinic light. **a** and **b** Rise (**a**) and decay (**b**) times for the bioluminescence intensity to change by 50% when turning actinic light on and off, respectively. Values were calculated based on the induction kinetics from the first and second cycles of luminescence of coelenterazine h–injected Nano-lantern(ATP1)–expressing WT (line 2: Supplemental Fig. S1a) and *pgr5* mutant (lines 1

and 3: Supplemental Fig. S1a) leaves, as shown in Figure 2. Asterisks indicate values that were significantly different (*$P < 0.05$; Student's *t*-test). Data representing means ± SD (n = 3).

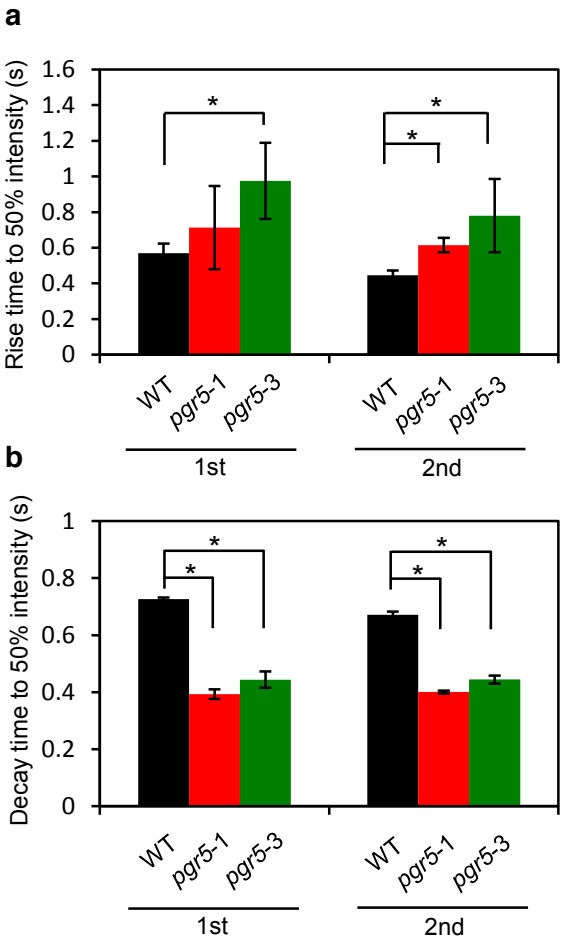
Click here to download Colour figure Fig1_rev.tif



Click here to download Line figure Fig2.tif



Click here to download Colour figure Fig3.pptx



Supplementary Figures

Click here to access/download
Supplementary material
Masuda_SupFigs.pdf

Supplementary Movie

Click here to access/download
Supplementary material
Supplementary movie 1.mov